Ukrainian Journal of Physical Optics
ISSUE 2
2024

NUMERICAL CALCULATION OF EFFECTIVE AREA OF FUNDAMENTAL MODE OF PHOTONIC CRYSTAL FIBERS

S. COSKUN [1], Y. OZTURK [2]

[1] Ege Vocational High School, Ege University, Bornova, İzmir-35100, Turkey, seyhan.coskun@ege.edu.tr
[2] Department of Electrical and Electronics, Faculty of Engineering, Ege University, Bornova, İzmir-35100, Turkey

Received: 26.12.2023

Abstract. The fundamental mode effective area of photonic crystal fiber (PCF) is calculated numerically using the cubic polynomial correction function as the correction factor of Marcuse and Petermann II equations. The numerical calculations are implemented using modified Marcuse and Petermann II methods for six different PCFs in the 1–2 μm wavelength range. The full-vectorial finite element method-based simulations are utilized to determine the effective area and coefficients of the cubic polynomial functions. After using the correction functions, by comparing the calculated effective area values with the values from the simulations, residuals of correction are obtained in the range of -1.11×10^{-3} μm² – $+2.66\times10^{-3}$ μm² and -1.4×10^{-3} μm² – $+5.112\times10^{-3}$ μm² respectively. These low residual values indicate that the offered method can be used successfully to calculate the wavelength-dependent effective mode area of PCFs in the investigated wavelength range without using simulations and complex theory.

Keywords: photonic crystal fiber, effective area, mode field diameter, correction function
UDC: 681.7
DOI: 10.3116/16091833/Ukr.J.Phys.Opt.2024.02069

1. Introduction

Photonic crystal fibers (PCFs) are an important milestone in developing optical fibers, which have been utilized for decades due to their superior transmission properties compared to copper lines in communication networks [1, 2]. PCFs, produced from a single material, contain holes enclosed in the fiber cladding, arranged periodically/aperiodically, and parallel to the fiber axis. Compared to conventional fibers, PCFs have very beneficial properties [3-5] depending on changes in their geometry. They can theoretically be designed as single-mode with infinite bandwidth [2, 4]. PCFs' dispersion, birefringence, and nonlinearity properties can be tuned to required values with appropriate geometric designs [6]. Additionally, PCFs have low bending losses [1-7].

There are several modeling methods for examining modes and mode properties in PCFs, such as the effective index approach [2, 8-12], plane-wave expansion (PWE) method [8, 9], localized-function method (LFM) [9, 12], multipole method (MM) [8, 9], beam propagation method (BPM) [8, 9], finite-difference method (FDM) [8, 13], finite-difference time-domain method (FDTD) [8, 9] and finite-element method (FEM) [8, 9, 14, 15]. As widely recognized in various research fields, FEM is also reliably used in PCFs as it has flexible and effective features [15].

The effective mode area, which is one of the significant characteristics of the fundamental mode in optical fibers, is essential in terms of dispersion [16], nonlinearity [17], splicing and bending losses [18], and confinement loss (an inherent feature of PCFs) [19].

If the fundamental mode is restricted in the core region and has a small area, nonlinear effects appear because the effective area and non-linear coefficient are inversely proportional. Non-linear PCFs are exploited in many optical non-linear processes. Supercontinuum generation in PCF has recently become a prominent research field of non-linear effects [20-22].

In order to meet the need for very high bit rates in optical communication networks, studies are carried out on very high-capacity fibers with wavelength division multiplexed and space division multiplexed [23]. In high-capacity fibers of long-haul communication, due to the summing of many multiplexed channels, transporting high power density of light causes nonlinear effects in fibers [24]. Therefore, the effective area must be large enough. Since the non-linearity parameter must be calculated at small wavelengths for addressing the non-linearity problem [25], and additionally, the critical radius must be taken into consideration for the bend loss problem at both small wavelengths and large wavelengths [2], the effective area value depending on the wavelength must be accurately determined in optical fibers that carry high power light in transmission fibers of communication networks. Again, a large effective area in the fiber optics is favored to avoid these nonlinear effects, provided that care is taken not to increase bending losses [26].

The effective mode area is a critical parameter in many PCF applications. For example, in fiber lasers and fiber amplifiers, the power is desired to be delivered with low nonlinearity, so the mode area should be calculated accurately. Considering the importance of the PCF effective area in various applications, such as communication and supercontinuum generation, research is conducted using established fiber theory as a milestone. As is well-known, for the circularly symmetric cylindrical step-index fibers (SIF), the fundamental mode's radial electric field distribution is considered Gaussian-shaped [27]. In this case, the mode field diameter (MFD) is used to calculate the effective mode area in SIFs [17]. Using similar approaches, numerous studies have been conducted to define and calculate the V-number, which is an important parameter for determining the PCF mode number and the mode area [8, 9, 12, 28]. Many studies, in particular, have focused on measuring and calculating the MFD and the effective area of the PCF fundamental mode. As one of the experimental studies, in the study of Miyagi et al., at a wavelength of 1.55 μm in some PCFs, MFD was measured by far-field scanning technique and found by simulations. The effective area values of PCFs have been calculated using the attained MFD values and correction factors at various values [17]. In addition, many studies were based on simulation, analytical, and numerical calculations. For example, Mortensen calculated PCF effective area numerically using a plane-wave basis model [29]. Nielsen et al. used numerical modeling to find effective index values and mode field radii in PCFs [30, 31]. Saitoh and Koshiba's FEM simulation revealed that MFD increases as the hole diameter to spacing ratio decreases in PCFs [9]. Sharma D. K. and Sharma A. employed an analytical field model to compare MFD values for various PCFs in the 0.4–0.75 μm wavelength range [32]. All these theoretical and experimental efforts in determining effective areas of PCFs give researchers insights and approximate calculation opportunities. Although there are well-developed empirical equations for PCFs [33] and approaches of Marcuse [30] and Petermann II [16, 34], it seems that there is still a need for numerical methods for PCFs. It is needed to contribute to the development of a numerical method for accurate calculation of PCF effective area in a wavelength range.

In this study, our work aims to perform numerical calculations using the Marcuse and Petermann II methods to calculate the effective area of the fundamental mode in PCFs over a broad wavelength range with relatively simple empirical equations. The effective area of the fundamental mode is simulated and numerically calculated for a total of six different solid-core PCFs made of silica glass, including two commercial ones. The calculations and simulations covered a wavelength range from 1 to 2 μm, using a package based on full-vectorial Finite Element Method (FEM). To determine the effective *V*-number of the PCFs, empirical relations Saitoh and Koshiba proposed [33] are employed in the numerical calculations. The effective areas of the PCFs are computed using Marcuse [30] and Petermann II definitions [16, 34] and a modified correction factor as a multiplier. In the numerical calculations for the PCFs, correction factors are established as cubic polynomial functions through data fitting. Following the implementation of these corrections using cubic polynomial functions, residuals are identified in the modified Marcuse and Petermann II methods for the PCFs. The rest of this paper is outlined as follows: Section 2 presents the methodology used in this study and the relevant fundamental theory. Section 3 provides the results, evaluations, and comparisons with previous studies. The study's conclusion is presented in Section 4.

2. Materials and Methods

For SIFs, the fundamental mode area can be approximately calculated, assuming that the shape of the fundamental mode is Gaussian. The fundamental mode area is calculated as a circular area using diameter (MFD of the fiber), the radial width of electric field distribution of guided single mode, taking the range between opposite e^{-1} = 0.37 field amplitude points in relation to the value at the fiber axis [27]. MFD can be measured by the spatial filtering technique, the transverse offset technique, the near-field scanning technique, and the far-field scanning technique [17, 18]. However, the electric field distribution of the fundamental mode is not exactly Gaussian in PCFs because of holes and the shape of hole rings (mostly hexagonal) in the cladding, as shown in Fig. 1. Therefore, the calculation of the mode area in PCFs must be different and is called effective mode area.

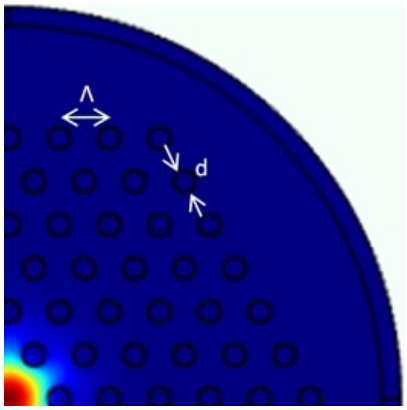

Fig. 1. Fundamental mode field distribution and geometry of the PCFs.

The effective mode area A_{eff} of the fundamental mode in PCFs can be calculated as

$$A_{eff} = k(\lambda)\pi\omega_{eff}^2, \quad (1)$$

where λ is the operating wavelength in vacuum, $k(\lambda)$ is the wavelength-dependent correction function, and ω_{eff} is mode field radius of the fundamental mode in the fibers, also called

effective modal spot size [35]. Petermann II and Marcuse approaches have been empirically developed for step index fibers. Although several effective parameters can be applied to calculate PCF with step index approaches, these parameters do not give the correct results for the A_{eff} because of the complex structure of the PCFs. Since the fundamental mode electric field distribution in conventional fibers (considering circular symmetry) is accepted as Gaussian, the effective mode field can be calculated as $\pi\omega_{eff}^2$ [17]. Due to the complex geometric structure of the claddings of the PCFs used in this study, the fundamental mode electric field distribution is not properly Gaussian, so a correction factor should be used to correct the calculations of the effective areas. In this study, instead of a constant of *k,* a correction function $k(\lambda)$ is used as differently from the previous study, where A_{eff} is calculated at a single wavelength [17]. Due to a correction constant not providing enough matching for every wavelength in a range of wavelengths, utilizing a correction function $k(\lambda)$ was preferred.

Marcuse and Petermann II empirical approaches are the most widely used methods for calculating the mode field radius in step-index fibers. Since core and cladding structures are different in PCFs from step-index fibers, several modifications must be adapted to use these methods. In general, instead of *V*-number, effective *V*-number [9], and instead of core radius, effective core radius is used to calculate the mode field radius with the Marcuse and Petermann II approaches for PCFs.

For PCF structure, as mentioned before, by using effective *V*-number [9], the effective mode field radius ω_{eff} can be calculated by the empirical Marcuse formula [30] for Gaussian field distribution as

$$\frac{\omega_{eff}}{a_{eff}} = 0.65 + \frac{1.619}{V_{eff}^{3/2}{}_{eff}} + \frac{2.879}{V_{eff}^6}, \tag{2}$$

where a_{eff} is effective core radius in the fiber, and V_{eff} is effective *V*-number.

A different method for calculating the radius of the fundamental mode that has a Gaussian field distribution is the Petermann II approach [16, 34]. In the study of Hussey et al [34], by combining Eqs. (1) and (2) and using V_{eff} instead of *V*, the formula for PCFs can be expressed as

$$\frac{\omega_{eff}}{a_{eff}} \approx 0.65 + \frac{1.619}{V_{eff}^{3/2}} + \frac{2.879}{V_{eff}^6} - \left(0.016 + \frac{1.561}{V_{eff}^7}\right). \tag{3}$$

In these Eqs. (2) and (3), the effective core radius of PCFs is calculated as [9]

$$a_{eff} = \frac{\Lambda}{\sqrt{3}}, \tag{4}$$

where Λ is the distance between the centers of two neighboring holes in the PCF cladding, as shown in Fig. 1.

In order to calculate V_{eff} included in Eqs. (2) and (3), effective indices of PCF modes must be determined. Finding the effective indices of core and cladding modes in PCF requires numerical modeling methods. Instead of finding the effective indices of PCF modes with enormous and time-consuming numerical calculations, a calculation method has been developed by Saitoh and Koshiba using some empirical relations [33]. By using this method, the *V*-number of PCF namely V_{eff}, can be calculated as [33]

$$V_{eff}\left(\frac{\lambda}{\Lambda}, \frac{d}{\Lambda}\right) = A_1 + \frac{A_2}{1 + A_3 \exp\left(A_4 \lambda / \Lambda\right)}. \tag{5}$$

The coefficients A_i in Eq. (5) are calculated as [33]

$$A_i = a_{i0} + a_{i1}\left(\frac{d}{\Lambda}\right)^{b_{i1}} + a_{i2}\left(\frac{d}{\Lambda}\right)^{b_{i2}} + a_{i3}\left(\frac{d}{\Lambda}\right)^{b_{i3}}. \quad (6)$$

In Eqs. (5) and (6), d is the diameter of holes, which is in the PCF cladding as shown in Fig. 1. In this study, the coefficients a_{ij} and b_{ij} in Eq. (6) are taken from the study of Saitoh and Koshiba [33].

The V_{eff} calculated in Eq. (5) is used in the Marcuse formula (Eq. (2)) and Petermann II definition (Eq. (3)) to calculate ω_{eff}. The A_{eff} values calculated with Eq. (1) and the A_{eff} values from the simulation are used to determine the $k(\lambda)$ correction function in Eq. (1).

In the FEM-based simulations, parameters related to the geometry of the PCFs (d, Λ, and fiber cladding diameter D) and the refractive index of silica glass, the material of which the PCFs are made, are used as input parameters. Both calculations and simulations use six different d/Λ ratios in the PCFs. The d/Λ ratios are 0.30, 0.40, ~0.44,~ 0.46, 0.50, and 0.60, respectively, and the PCFs are named based on this order as PCF-i (i = 1 to 6). PCF-3 and PCF-4 at ratios of 0.4374 and 0.46154 here belong to commercial products ESM-12B and LMA-10, respectively. There are 126 holes in the cladding of the PCFs, and they are arranged as six concentric hexagonal rings. The cladding diameter D is 125 μm in all the PCFs. The distance between two holes in the claddings is 8 μm in all PCFs except PCF-4, where this value is 6.5 μm. In the simulations, a perfectly matched layer (PML) is used as the outermost layer of the PCFs. FEM-based methods have been applied to PCF structures in many studies due to their advantages in terms of accuracy [15]. However, they require numerous and complex numerical calculations or access to high-cost programming platforms. With the help of FEM-based simulations, the final results of the study are straightforward and can be used to calculate the effective area of several PCFs using relatively simple analytical equations.

3. Results and Discussion

Effective V-number (V_{eff}) values for six different solid-core PCFs are calculated at various wavelengths within the 1–2 μm of wavelength range using the Eqs. (5) and (6). The effective area A_{eff} of the fundamental mode is determined by finding the effective mode field radius, which is obtained through the Marcuse and Petermann II relations given by Eqs. (2) and (3). Additionally, in the A_{eff} calculations from Marcuse and Petermann II, at first the correction factor $k(\lambda)$ is taken as 1 ($k(\lambda)$=1). Additionally, with the simulation based on full-vector FEM, the effective area of the fundamental mode in these PCFs was found for various wavelengths.

The wavelength-dependent variations of the A_{eff} values obtained through three different methods for six different PCFs are shown in Fig. 2. A_{eff} values are plotted against wavelengths in Fig. 2 while keeping the $k(\lambda)$ constant at 1 to show the importance of the correction function. Obviously, both of the results for the Marcuse and Petermann II approaches differ from the results found with FEM, as shown in Fig. 2.

While it is possible to use a constant instead of a correction function at a single wavelength, as seen in the study of Miyagi et al. [17], it is not sufficient for the entire wavelength range investigated in this study. The required correction functions for A_{eff} values calculated at some wavelengths with Marcuse and Petermann II approaches for each PCF are determined as relative values for the FEM results. The relative effective area values ($k(\lambda)$ values) are obtained by dividing the Marcuse and Petermann II values by the simulation values.

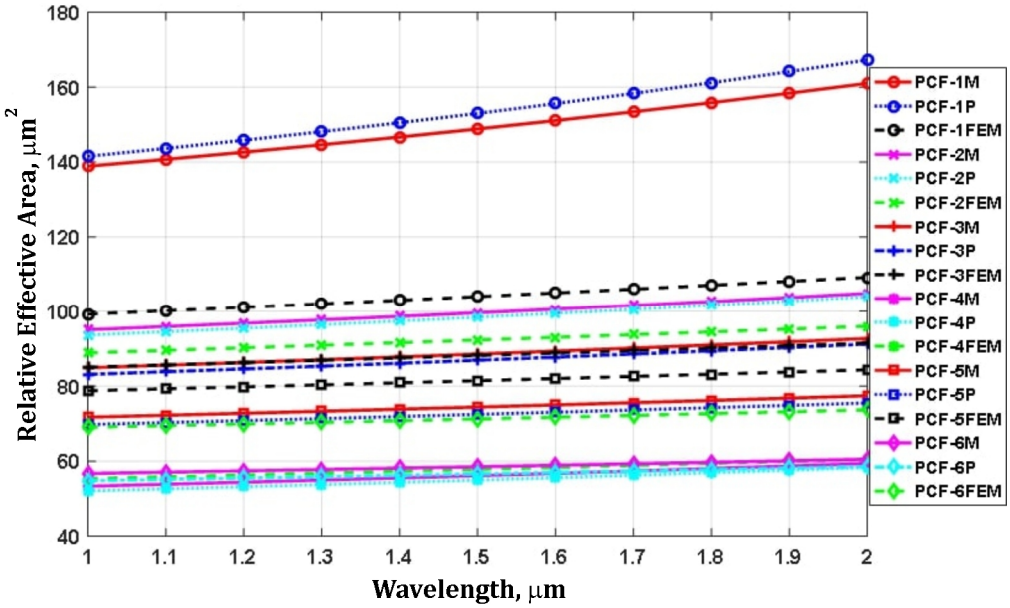

Fig. 2. Variations of the effective area found in the six PCFs with 3 methods as a function of wavelength. $k(\lambda)$= 1.0. M - Marcuse method, P - Petermann II method.

Similar to conventional fibers, A_{eff} in PCFs varies with wavelength. Additionally, as seen in Fig. 2, the wavelength dependence of the A_{eff} values varies with d/Λ values. Apparently, due to the complex geometry of PCFs, the correction function is expected to also depend on wavelength. The correction functions are chosen as cubic polynomials due to being simple while fitting significantly well to the relative A_{eff} values with minimum residuals. If the linear functions are used for the correction, very large residuals reaching 70% are obtained. Quadratic functions could also be considered, but it is observed that cubic functions resulted in lower residuals. The graphs of the wavelength-dependent $k(\lambda)$ values found with the two methods for PCF-2 are shown in Fig. 3. The General expression of the wavelength-dependent correction function is as follows

$$k(\lambda) = A\lambda^3 + B\lambda^2 + C\lambda + D\,. \tag{7}$$

The coefficients in the cubic polynomial functions (A, B, C, D) given in Eq. (7) are determined and provided in Table 1 for all PCFs and the methods employed in the study. Fig. 3 and 4 present the results only for PCF-2 (d/Λ = 0.4) for the purpose of clarity and simplicity. From Fig. 3, the $k(\lambda)$ values fall within the range of 0.916 to 0.935 for the Marcuse method and 0.923 to 0.949 for the Petermann II method within the studied wavelength range.

The effective area calculated with the presented method and, previously, Mortensen's numerical calculation [29] with the plane wave basis model can be compared. For example for 1550 nm wavelength and (d/Λ=0.46, Λ=6.5 μm) our method gives 57 μm² but Mortensen's are around ~55 μm². When the results obtained in two different studies are compared, they are found to be compatible. After applying corrections to the values obtained with Marcuse and Petermann II methods, wavelength dependent effective area values are plotted for PCF-2 as shown in Fig. 4. In Fig. 4, it is apparent that the three curves for A_{eff}, calculated using three different methods completely overlap.

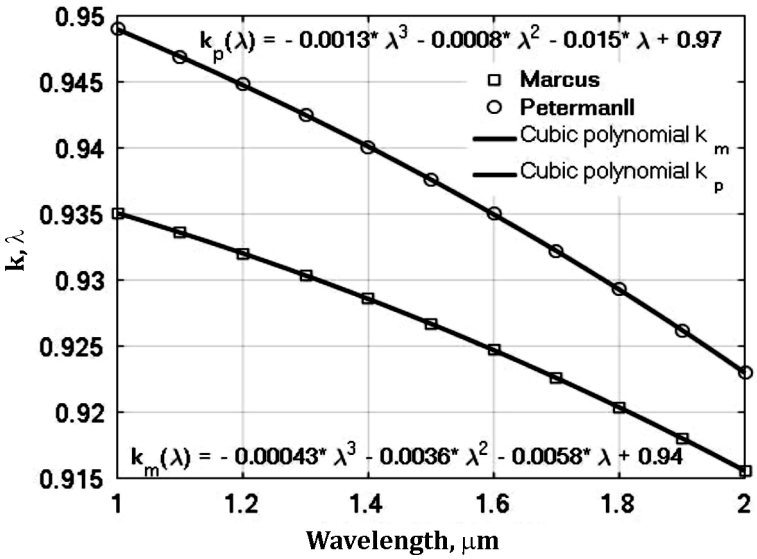

Fig. 3. Wavelength-dependent changes of the $k(\lambda)$ obtained by the Marcuse and Petermann II methods for PCF-2.

In Fig. 4 inset, the difference between the results found after applying corrections with the Marcuse and Petermann II methods and the results obtained with FEM is presented as the residuals of correction. In the inset of Fig. 4, for the Marcuse and Petermann II methods, effective area residuals vary between -1.11×10^{-3} to $+2.66\times10^{-3}$ μm^2 and -1.4×10^{-3} to $+5.112\times10^{-3}$ μm^2, respectively.

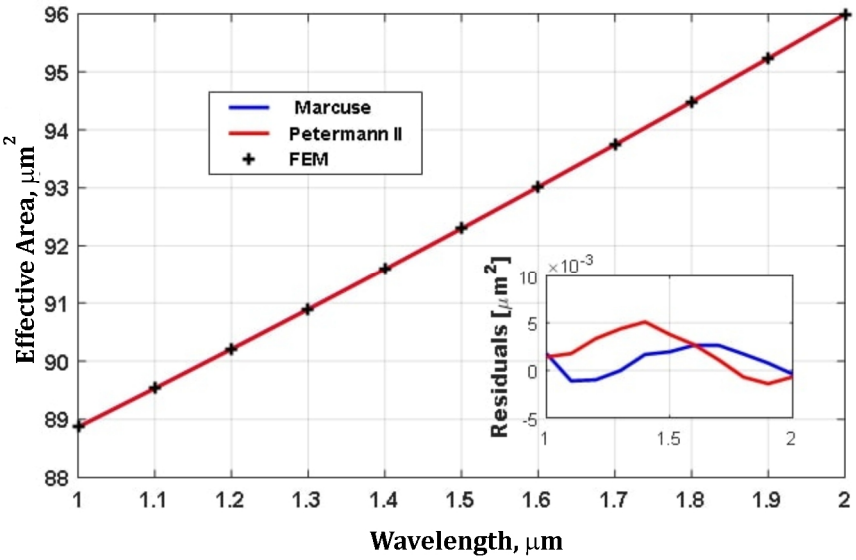

Fig. 4. Effective area versus wavelength after correction for PCF-2 for the 3 methods. Inset: correction residuals for both methods.

For six PCFs and the two methods, coefficients and the norm of residuals of the $k(\lambda)$ are given in Table 1. As seen in Table 1, for cubic polynomial correction functions selected for the PCFs, the norm of residuals take values in the range of 2.77×10^{-5}–15.87×10^{-5}. In their study, Sharma D. K. and Sharma A. used various MFD calculation methods for some PCFs

[32]. When A_{eff} is calculated, it was seen that there is a difference of 55.2×10^{-3} μm^2 in two different methods with the closest values in a PCF [32]. At the same time, the difference between numerical and experimental results in the study of Miyagi et al. has been given at a single wavelength of 10×10^{-3} μm^2 [17]. In our study, we have chosen the correction function cubic polynomial to have much smaller residuals in the wavelength range.

Table 1. Coefficients of cubic polynomial correction functions.

PCF	Method	A	B	C	D	NRCP*, 10^{-5}
PCF-1	Marcuse	0.0002137	-0.01039	-0.007027	0.7317	7.867
	Petermann II	-0.0004662	-0.008695	-0.01927	0.7295	9.362
PCF-2	Marcuse	-0.0004274	-0.003555	-0.005848	0.9449	7.57
	Petermann II	-0.001263	-0.0007984	-0.01477	0.9658	5.943
PCF-3	Marcuse	-0.001238	0.001211	-0.00997	1.012	2.77
	Petermann II	-0.001344	0.0008467	-0.01319	1.037	2.82
PCF-4	Marcuse	0.00003885	-0.008275	0.004074	1.043	14.91
	Petermann II	-0.0008159	-0.005594	-0.003992	1.073	15.87
PCF-5	Marcuse	-0.001632	0.004569	-0.01107	1.106	7.6
	Petermann II	-0.001865	0.005221	-0.0148	1.141	7.82
PCF-6	Marcuse	-0.001554	0.006235	-0.01026	1.222	10.8
	Petermann II	-0.001437	0.006107	-0.008718	1.266	11.18

NRCP* - Norm of residuals for cubic polynomial.

Table 2. The optimal correction constants of the PCFs used to concur A_{eff} values calculated with the 3 methods at the wavelength of 1500 nm.

	k correction constants		Minimum and maximum values of A_{eff}			Maximum residuals	
PCF	M*	P**	Marcuse	Petermann II	FEM	Marcuse	Petermann II
PCF-1	0,582	0,566	97,00127512	96,14559868	99,239	-2,237724877	-3,093401323
			112,4803548	113,6407346	109,17	3,310354839	4,470734635
PCF-2	0,7721	0,7811	88,05766188	87,77969626	88,872	-0,814338121	-1,092303735
			97,14504516	97,49000786	95,996	1,149045164	1,494007855
PCF-3	0,9956	1,0145	84,50092387	84,31888404	85,036	-0,535076133	-0,717115964
			92,29072226	92,52667697	91,484	0,806722257	1,04267697
PCF-4	1,0304	1,052	54,9580718	54,8218744	55,385	-0,426928205	-0,563125599
			61,22389904	61,39672475	60,48	0,743899038	0,916724754
PCF-5	1,0942	1,124	78,47096261	78,39742486	78,753	-0,282037386	-0,35557514
			84,70776909	84,86599923	84,331	0,376769089	0,534999226
PCF-6	1,21734	1,25882	69,04895646	68,99342111	69,053	-0,004043535	-0,059578888
			73,68283458	73,73958432	73,66	0,02283458	0,079584322

*M - Marcuse, P** - Petermann II

In order to examine the situation where the correction factor is taken as a constant, the $A_{eff}(\lambda)$ values found by the Marcuse and Petermann II methods in each PCF were multiplied by optimum constants. These graphs coincided at the wavelength of 1500 nm, which is the middle of the spectrum, with the graphs found by FEM.

A_{eff} values found with these calculations are given in Table 2. Additionally, the residuals at the extreme points of the spectrum are also given in the table. As seen in the Table 2, if the correction factor is taken as an optimum constant, the residuals decreases as the d/Λ value increases.

In comparison of the cubic polynomial correction function and correction constant, as seen in Table 1 and Table 2, the function residuals appear to be at least 1000 times smaller than those of the constants.

4. Conclusion

In this study, the effective area values in 6 different PCFs that have non-Gaussian fundamental mode fields have been calculated as a function of wavelength using the Marcuse and the Petermann II methods within a wavelength range of 1–2 μm. In these calculations carried out with Eq. (1), it is shown that it is more appropriate to use the correction function instead of the correction constant for more quantitatively accurate calculations in a wavelength range. Cubic polynomials are selected as the correction functions for A_{eff} calculations of the PCFs.

It is shown that, instead of enormous numerical calculations of numerical PCF modeling methods, the fundamental mode area in PCF is calculated numerically using the modified Marcuse and Petermann II methods along with a cubic polynomial correction function. When this correction function is used, the norm of residuals falls within the range of 2.77×10^{-5}–15.87×10^{-5} for all PCFs and both methods. After the corrections are implemented, residuals of corrections are found in Marcuse and Petermann II methods for the PCF-2 as varying between -1.11×10^{-3} to $+2.66\times10^{-3}$ μm^2 and -1.4×10^{-3} to $+5.112\times10^{-3}$ μm^2, respectively. Based on these results, it is found that the designation of a cubic polynomial function of wavelength as a correction factor is highly suitable for calculating the A_{eff}. It is not only simple but also demonstrates a remarkable fit to the relative A_{eff} values, resulting in minimal residuals.

Optimizing A_{eff} in fiber optics, particularly in the context of endlessly single-mode bandwidth PCFs, is expected to be a critical issue in the future of communication networks. As a direct and simple method, our calculation approach on PCF fundamental mode area, which works in a wavelength range, can serve as a valuable tool for studies in future PCF research.

Disclosures. The authors declare no conflict of interest.

References

1. Knight, J. C., Birks, T. A., Russell, P. S. J., & Atkin, D. M. (1996). All-silica single-mode optical fiber with photonic crystal cladding. *Optics Letters*, *21*(19), 1547-1549.
2. Birks, T. A., Knight, J. C., & Russell, P. S. J. (1997). Endlessly single-mode photonic crystal fiber. *Optics Letters*, *22*(13), 961-963.
3. Broeng, J., Mogilevstev, D., Barkou, S. E., & Bjarklev, A. (1999). Photonic crystal fibers: A new class of optical waveguides. *Optical Fiber Technology*, *5*(3), 305-330.
4. Knight, J. C., Birks, T. A., Cregan, R. F., Russell, P. S. J., & De Sandro, J. P. (1999). Photonic crystals as optical fibres–physics and applications. *Optical Materials*, *11*(2-3), 143-151.
5. Russell, P. (2003). Photonic crystal fibers. *Science*, *299*(5605), 358-362.

6. Russell, P. S. J. (2006). Photonic-crystal fibers. *Journal of Lightwave Technology*, *24*(12), 4729-4749.
7. Saitoh, K., Koshiba, M., Hasegawa, T., & Sasaoka, E. (2003). Chromatic dispersion control in photonic crystal fibers: application to ultra-flattened dispersion. *Optics express*, *11*(8), 843-852.
8. Buczynski, R. J. A. P. P. S. A. (2004). Photonic crystal fibers. *Acta Physica Polonica A*, *106*(2), 141-167.
9. Saitoh, K., & Koshiba, M. (2005). Numerical modeling of photonic crystal fibers. *Journal of Lightwave Technology*, *23*(11), 3580-3590.
10. Li, Y. F., Wang, C. Y., & Hu, M. L. (2004). A fully vectorial effective index method for photonic crystal fibers: application to dispersion calculation. *Optics Communications*, *238*(1-3), 29-33.
11. Li, Y., Yao, Y., Hu, M., Chai, L., & Wang, C. (2008). Improved fully vectorial effective index method for photonic crystal fibers: evaluation and enhancement. *Applied Optics*, *47*(3), 399-406.
12. Mogilevtsev, D., Birks, T. A., & Russell, P. S. J. (1999). Localized function method for modeling defect modes in 2-D photonic crystals. *Journal of lightwave technology*, *17*(11), 2078.
13. Zhu, Z., & Brown, T. G. (2002). Full-vectorial finite-difference analysis of microstructured optical fibers. *Optics Express*, *10*(17), 853-864.
14. Kim, B., Kim, H. M., Naeem, K., Cui, L., Chung, Y., & Kim, T. H. (2010). Design, fabrication, and sensor applications of photonic crystal fibers. *Journal of the Korean Physical Society*, *57*(6), 1937-1941.
15. Bréchet, F., Marcou, J., Pagnoux, D., & Roy, P. J. O. F. T. (2000). Complete analysis of the characteristics of propagation into photonic crystal fibers, by the finite element method. *Optical Fiber Technology*, *6*(2), 181-191.
16. Petermann, K. (1983). Constraints for fundamental-mode spot size for broadband dispersion-compensated single-mode fibres. *Electronics Letters*, *18*(19), 712-714.
17. Miyagi, K., Namihira, Y., Razzak, S. A., Kaijage, S. F., & Begum, F. (2010). Measurements of mode field diameter and effective area of photonic crystal fibers by far-field scanning technique. *Optical Review*, *17*, 388-392.
18. Artiglia, M., Coppa, G., Di Vita, P., Potenza, M., & Sharma, A. (1989). Mode field diameter measurements in single-mode optical fibers. *Journal of Lightwave Technology*, *7*(8), 1139-1152.
19. Coşkun, S., Öztürk, Y., & Kahraman, G. (2018). Applied magnetic field effect on core mode properties of MFPCF. *Micro & Nano Letters*, *13*(9), 1306-1309.
20. Wadsworth, W. J., Ortigosa-Blanch, A., Knight, J. C., Birks, T. A., Man, T. P. M., & Russell, P. S. J. (2002). Supercontinuum generation in photonic crystal fibers and optical fiber tapers: a novel light source. *JOSA B*, *19*(9), 2148-2155.
21. Dudley, J. M., Genty, G., & Coen, S. (2006). Supercontinuum generation in photonic crystal fiber. *Reviews of Modern Physics*, *78*(4), 1135.
22. Saghaei, H., Moravvej-Farshi, M. K., Ebnali-Heidari, M., & Moghadasi, M. N. (2015). Ultra-wide mid-infrared supercontinuum generation in As 40 Se 60 chalcogenide fibers: solid core PCF versus SIF. *IEEE Journal of Selected Topics in Quantum Electronics*, *22*(2), 279-286.
23. Morioka, T., Awaji, Y., Enami, K., Miyamoto, Y., Morita, I., Okumura, Y., Suzuki, M., Takara, H., Terada, J., and Yamamoto, K. (2022). Introduction. In: *Space-division multiplexing in optical communication systems, extremely advanced optical transmission with 3M technologies*, Nakazawa M., Suzuki M., Awaji Y., Morioka T. (Eds.), Springer, Cham.
24. Hamaoka, F., Nakamura, M., Okamoto, S., Minoguchi, K., Sasai, T., Matsushita, A., Yamazaki, E. & Kisaka, Y. (2019). Ultra-wideband WDM transmission in S-, C-, and L-bands using signal power optimization scheme. *Journal of Lightwave Technology*, *37*(8), 1764-1771.
25. Agrawal, G. (2019). *Nonlinear fiber optics*. (6th ed.), Elsevier. https://shop.elsevier.com/books/nonlinear-fiber-optics/agrawal/978-0-12-817042-7.
26. Downie, J.D., Li, M.J., Makovejs, S. (2019). *Single-mode fibers for high speed and long-haul transmission.* In: Peng, GD. (Eds.) Handbook of Optical Fibers. Springer, Singapore.
27. Senior, J. M., & Jamro, M. Y. (2009). *Optical fiber communications: principles and practice*. Pearson Education.
28. Mortensen, N. A., Folkenberg, J. R., Nielsen, M. D., & Hansen, K. P. (2003). Modal cutoff and the V parameter in photonic crystal fibers. *Optics Letters*, *28*(20), 1879-1881.
29. Mortensen, N. A. (2002). Effective area of photonic crystal fibers. *Optics Express*, *10*(7), 341-348.
30. Marcuse, D. (1977). Loss analysis of single-mode fiber splices. *Bell System Technical Journal*, *56*(5), 703-718.
31. Nielsen, M. D., Mortensen, N. A., Folkenberg, J. R., & Bjarklev, A. (2003). Mode-field radius of photonic crystal fibers expressed by the V parameter. *Optics Letters*, *28*(23), 2309-2311.
32. Sharma, D. K., & Sharma, A. (2013). On the mode field diameter of microstructured optical fibers. *Optics Communications*, *291*, 162-168.
33. Saitoh, K., & Koshiba, M. (2005). Empirical relations for simple design of photonic crystal fibers. *Optics Express*, *13*(1), 267-274.
34. Hussey, C. D., & Martinez, F. (1985). Approximate analytic forms for the propagation characteristics of single-mode optical fibres. *Electronics Letters*, *23*(21), 1103-1104.
35. Koshiba, M., & Saitoh, K. (2004). Applicability of classical optical fiber theories to holey fibers. *Optics Letters*, *29*(15), 1739-1741.

S. Coskun, Y. Ozturk (2024). Numerical Calculation of Effective Area of Fundamental Mode of Photonic Crystal Fibers. *Ukrainian Journal of Physical Optics*, *25*(2), 02069 – 02079.
doi: 10.3116/16091833/Ukr.J.Phys.Opt.2024.02069

Анотація. *Чисельно розрахована ефективна площа основної моди фотонного кристалічного волокна (ФКВ) за допомогою кубічної поліноміальної корекційної функції, як поправочного коефіцієнта рівнянь Маркузе та Петермана II. Чисельні розрахунки виконані з використанням модифікованих методів Маркузе та Петермана II для шести різних ФКВ в діапазоні довжин хвиль 1–2 мкм. Моделювання на основі повного векторного методу скінченних елементів використовуються для визначення ефективної площі та коефіцієнтів кубічних поліноміальних функцій. Після використання корекційних функцій шляхом порівняння розрахованих значень ефективної площі зі значеннями з моделювання отримано залишки корекції в діапазоні* $-1{,}11\times10^{-3}$ *мкм²* $-$ $+2{,}66\times10^{-3}$ *мкм²* *та* $-1{,}4\times10^{-3}$ *мкм²* $-$ $+5{,}112\times10^{-3}$ *мкм², відповідно. Такі низькі значення залишків вказують на те, що запропонований метод може бути успішно використаний для розрахунку залежної від довжини хвилі ефективної площі моди ФКВ у досліджуваному діапазоні довжин хвиль без використання моделювання та складної теорії.*

Ключові слова: *фотонно-кристалічне волокно, ефективна площа, діаметр поля моди, функція корекції*